J. Fluid Mech. (1991), *vol.* 233, *pp.* 329–347
Printed in Great Britain

Nonlinear dynamics near the stability margin in rotating pipe flow

By Z. YANG† AND S. LEIBOVICH
Sibley School of Mechanical and Aerospace Engineering, Cornell University, Ithaca, NY 14853, USA

(Received 4 December 1990 and in revised form 5 June 1991)

The nonlinear evolution of marginally unstable wave packets in rotating pipe flow is studied. These flows depend on two control parameters, which may be taken to be the axial Reynolds number R and a Rossby number, q. Marginal stability is realized on a curve in the (R, q)-plane, and we explore the entire marginal stability boundary. As the flow passes through any point on the marginal stability curve, it undergoes a supercritical Hopf bifurcation and the steady base flow is replaced by a travelling wave. The envelope of the wave system is governed by a complex Ginzburg–Landau equation. The Ginzburg–Landau equation admits Stokes waves, which correspond to standing modulations of the linear travelling wavetrain, as well as travelling wave modulations of the linear wavetrain. Bands of wavenumbers are identified in which the nonlinear modulated waves are subject to a sideband instability.

1. Introduction

Although instability and transition to turbulence for flow in a pipe was observed by Reynolds (1883) more than a century ago, the phenomenon remains without theoretical explanation. This is mainly because the flow appears to be linearly stable at all Reynolds numbers, as suggested by the results of Gill (1965), Salwen & Grosch (1972), and others. The observed instability is consequently attributed to so-far unexplained nonlinear effects. Although weakly nonlinear analyses of this problem have been attempted (see Davey & Nguyen 1971; Itoh 1977; and Davey 1978) objections to these procedures can be raised because there is no linear neutral stability point about which a rational amplitude expansion can be carried out (Herbert 1983). Numerical simulations by Patera & Orszag (1981) demonstrate, at least for axisymmetric perturbations, that the amplitude expansions constructed without benefit of a neutral curve are not valid for this problem. Direct simulations allowing for three-dimensional perturbations (Orszag & Patera 1983) have proved less illuminating in this problem than corresponding computations for problems, such as plane Poiseuille flow, which *do* enjoy a neutral curve.

Rotation of the pipe changes the picture entirely. In this case, Pedley (1968, 1969), and simultaneously Joseph & Carmi (1969) showed that the superposition of rigid rotation – absolutely stable by itself – with ordinary circular Poiseuille flow, also stable, can lead to instability if the rotation rate is high. Mackrodt (1976) later suggested that the observed transition in non-rotating pipe flow is due to residual swirl in the fluid entering the pipe. He extended previous linear stability results to

† Present address: Center for Modeling of Turbulence and Transition, NASA Lewis Research Center/ICOMP, Cleveland, OH 44135, USA.

small rotation rates, and showed, both theoretically and experimentally, that pipe flow can be linearly unstable in this regime. For large Reynolds number, he found that the rotation needed to render the flow unstable is inversely proportional to the Reynolds number. He suggested that the effect of entering swirl might have escaped experimental observation since the swirl rate needed to destabilize the flow is small for large Reynolds number.

Since there exists a stability margin for the flow in the rotating pipe – about which there is now a great deal known, thanks to the comprehensive linear stability analysis of Cotton & Salwen (1981) – one can formulate a rational weakly nonlinear analysis for the evolution of the marginally unstable perturbation. Akylas & Demurger (1984) treated the weakly nonlinear stability for flow in the rotating pipe by an amplitude expansion technique following the analysis of Stuart (1960) and Watson (1960) for plane Poiseuille flow. Their aim was to find out if the bifurcation was subcritical or supercritical. If the bifurcation were subcritical, the observed transition to turbulence in the non-rotating pipe flow might be due to the unstable solution subcritically bifurcating from the flow in a rotating pipe. Their numerical results, which had indicated subcritical bifurcation, were in error, as pointed out by Toplosky & Akylas (1988), and by Mahalov & Leibovich (1989, 1991). Toplosky & Akylas (1988) numerically computed fully nonlinear solutions to the rotating pipe flow in the special case of helical waves. Landman (1990) has extended these fully nonlinear solutions to highly supercritical regimes, and has found two-frequency solutions, a series of period-doubling bifurcations, and apparently chaotic solutions. The helical waves in these studies are two-dimensional solutions, constant on helices at each radial location, and periodic in the axial direction: mathematical properties of these solutions have been discussed by Mahalov, Titi & Leibovich (1990).

Our study is a generalization of that of Akylas & Demurger (1984) and parallels that of Stewartson & Stuart (1971) who analysed the evolution of wave systems in plane Poiseuille flow. We study the nonlinear evolution of a wave packet in the vicinity of the entire marginal stability boundary in the (R, q)-plane. The direction and nature of the bifurcation is determined, and it is found that the bifurcation is supercritical everywhere. The governing equation for the amplitude of the wave system, allowing for spatial modulation, is a Ginzburg–Landau equation with complex coefficients. Travelling wave solutions of the Ginzburg–Landau equation are found and the stability of the solutions to sideband perturbations is analysed along the (entire) marginal stability curve.

The plan of this study is as follows. In §2, we formulate the problem. The results from linear stability analysis needed in carrying out the weakly nonlinear analysis are described in §3. A weakly nonlinear expansion using a multiscale technique is carried out in §4, which leads to a complex Ginzburg–Landau equation for the perturbation envelope. Modulated travelling wave solutions of the Ginzburg–Landau equation and the stability are discussed in §5, and §6 concludes the paper.

2. Problem formulation

If length is non-dimensionalized by the radius of the pipe L and velocity by the axial velocity at the axis U, the laminar base flow in a pipe rotating with angular velocity Ω is then described in a cylindrical (z, θ, r) coordinate system by

$$U = (1-r^2, qr, 0), \tag{1}$$

where

$$q = \Omega L/U \tag{2}$$

measures the relative strength of rotation. This non-dimensionalization also defines a Reynolds number

$$R = UL/\nu, \tag{3}$$

where ν is the kinematic viscosity of the fluid. Thus, the base flow in a rotating pipe is characterized by (R, q).

Writing the instantaneous velocity field as the sum of the base flow and the perturbation field

$$\boldsymbol{v} = \boldsymbol{U} + \boldsymbol{u},$$

the Navier–Stokes equation and the equation of continuity requires the perturbation field $\hat{\boldsymbol{u}} = (u, v, w; p)$, where p is the pressure perturbation, to satisfy the following equation:

$$\mathbf{L}\left(\frac{\partial}{\partial t}, \frac{\partial}{\partial z}, \frac{\partial}{\partial \theta}, \frac{\partial}{\partial r}; R, q\right)\hat{\boldsymbol{u}} = \mathbf{N}(\hat{\boldsymbol{u}}, \hat{\boldsymbol{u}}), \tag{4}$$

where $\mathbf{L}$ is the linear part of the differential operator, and $\mathbf{N}$, which is quadratic in perturbation velocity, is the nonlinear part of the differential operator. $\mathbf{L}$ is a 4×4 matrix, and $\mathbf{N}$ is a 4×1 vector. The entries of $\mathbf{L}$ and $\mathbf{N}$ in a cylindrical coordinate system are listed in Appendix A.

The perturbation field should satisfy the no-slip condition at the wall of the pipe and the uniqueness and regularity conditions at the centre of the pipe.

3. Temporal linear stability analysis

Linear stability is governed by (4) with the right-hand side neglected,

$$\mathbf{L}\left(\frac{\partial}{\partial t}, \frac{\partial}{\partial z}, \frac{\partial}{\partial \theta}, \frac{\partial}{\partial r}; R, q\right)\hat{\boldsymbol{u}} = 0. \tag{5}$$

Since the problem is separable in the z- and θ-directions, the perturbation field may be written in normal mode form, i.e.

$$\begin{aligned}\hat{\boldsymbol{u}} &= A\boldsymbol{\varphi}E \\ &\equiv A[u(r), v(r), w(r), p(r)] \exp[\mathrm{i}(kz + m\theta - \omega t)],\end{aligned}$$

where A is an arbitrary constant, k is the axial wavenumber of the perturbation and m is the azimuthal wavenumber of the perturbation; and ω is the complex frequency, with its real part being the frequency and the imaginary part being the growth rate. In a temporal stability analysis ω is regarded as an eigenvalue to be found; if $\mathrm{Im}\,(\omega)$ is positive, the flow is linearly unstable.

The normal mode assumption transforms the partial differential equations (5) to a set of ordinary differential equations given by

$$\mathbf{L}\left(-\mathrm{i}\omega, \mathrm{i}k, \mathrm{i}m, \frac{\partial}{\partial r}; R, q\right)\boldsymbol{\varphi} = 0. \tag{6}$$

The above equations for the perturbations are supplemented by the following boundary conditions. On the wall of the pipe, the no-slip boundary conditions require

$$u(1) = v(1) = w(1) = 0. \tag{7}$$

At the centre of the pipe, the perturbation must satisfy the following conditions to ensure that it be single-valued (see Batchelor & Gill 1962):

$$\left.\begin{aligned} &u'(0) = v(0) = w(0) = p'(0) = 0 \quad \text{for} \quad m = 0, \\ &u(0) = v(0) + imw(0) = p(0) = 0 \quad \text{for} \quad |m| = 1, \\ &u(0) = v(0) = w(0) = p(0) = 0 \quad \text{for} \quad m \quad \text{otherwise.} \end{aligned}\right\} \tag{8}$$

The ordinary differential equations and the boundary conditions form an eigenvalue problem with ω as the eigenvalue and φ as the eigenfunction. Non-trivial solutions exist only when ω takes some specific values given by

$$\omega = \omega(R, q; m, k).$$

Of the four parameters $(R, q; m, k)$, (R, q) specify the base flow and (m, k) specify the wavenumbers of the perturbation. For a given pair of control parameters (R, q) and for a given perturbation (m, k), if $\mathrm{Im}(\omega)$ is less than zero, the flow is stable to this particular perturbation; if $\mathrm{Im}(\omega)$ is positive, the flow is said to be linearly unstable to the perturbation. For a given pair of (R, q), if the flow is stable to all the possible combinations of m and k, the flow is said to be linearly stable (i.e. it is stable to infinitesimal perturbations.) The marginal linear stability curve, on which the growth rate of the most unstable perturbation is zero, separates the region in the (R, q)-plane where the flow is linearly stable from the region where it is linearly unstable.

We briefly review the main linear stability results found by Pedley (1969), Mackrodt (1976), and Cotton & Salwen (1981) with the emphasis on the most recent of these papers. When plotted on the (R, Rq) plane, unstable motion takes place essentially in the quarter plane $R > 83$, $\hat{\Omega} = Rq > 27$. The marginal stability boundaries are not precisely parallel to the $R, \hat{\Omega}$-axes, but are not far from being so. The minimum value of R for which instability is possible is 82.9, which is very close to the energy stability limit of Joseph & Carmi (1969) of 81.49. The minimum value of $\hat{\Omega}$ is 26.96, according to Mackrodt (1976), and occurs for $|k|R = 106.6$. The modes which first become unstable, as either R or $\hat{\Omega}$ is increased so as to cross from the stable to the unstable region, have $m = 1$.

Cotton & Salwen (1981) note that the symmetries of the problem imply that for any solution of the linear problem for a given set of the parameters $(R, q; m, k)$, there is a solution having the same time history but corresponding to a parameter set with the signs of any two of the parameters altered. Thus, there is no loss of generality in arbitrarily fixing R, q and m to be positive, while the sign of k is arbitrary. With this convention, instability has been found to be possible only when k is negative. We adopt the same convention.

A spectral method with Chebyshev polynomials as the basis functions is used in this study to numerically solve the differential equations. The velocity field and pressure are written as

$$\left.\begin{aligned} u(r) &= \sum_{i=1}^{N} u_i T_{i-1}(y), \quad v(r) = \sum_{i=1}^{N} v_i T_{i-1}(y), \\ w(r) &= \sum_{i=1}^{N} w_i T_{i-1}(y), \quad p(r) = \sum_{i=1}^{N} p_i T_{i-1}(y), \end{aligned}\right\} \tag{9}$$

where y is related to r by $y = 2r - 1$ so that the domain of definition for y is from -1 to 1. The reduction from the differential equations to a set of algebraic equations is made by a Galerkin–Tau projection. To eliminate the coordinate singularities at $r = 0$, Navier–Stokes equations were multiplied by r^2 and the equation of continuity was multiplied by r before the projection. The result of the discretization is the following generalized eigenvalue problem:

$$\boldsymbol{M}(-\mathrm{i}\omega; \mathrm{i}k, \mathrm{i}m; R, q)\,\boldsymbol{\Phi} = \boldsymbol{A}(R, q; m, k)\,\boldsymbol{\Phi} - \mathrm{i}\omega \boldsymbol{B}(R, q; m, k)\,\boldsymbol{\Phi} = 0 \tag{10}$$

where $\boldsymbol{\Phi} = (u_1, u_2, \ldots, u_N, v_1, v_2, \ldots, v_N, w_1, w_2, \ldots, w_N, p_1, p_2, \ldots, p_N)$. The entries of the complex matrices $\boldsymbol{A}$ and $\boldsymbol{B}$ are shown in Appendix B.

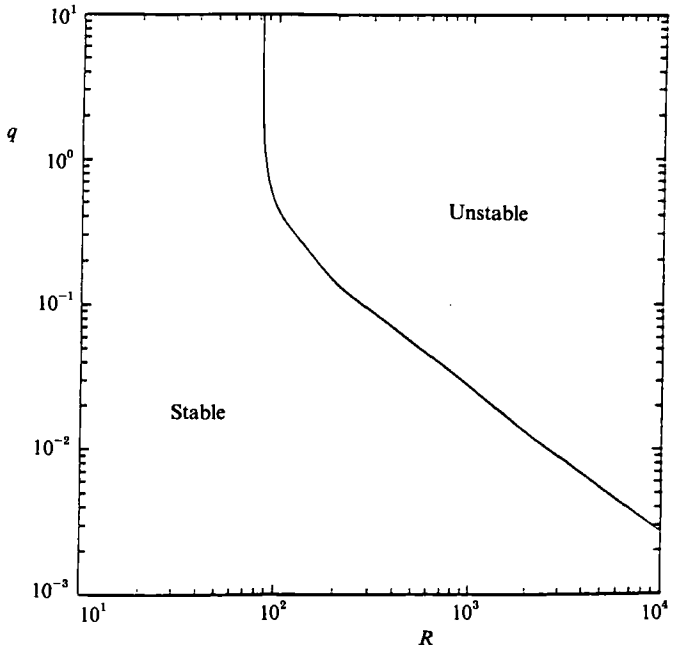

FIGURE 1. Marginal stability curve, showing linearly stable and unstable regions.

R	q	m	k	ω_i
156.0	0.2147	1	−1.0	0.33×10^{-4}
10700	0.00252	1	−0.01	0.17×10^{-5}
110.0	149.1	3	−0.01	-0.84×10^{-3}
23300	0.00300	3	−0.01	0.53×10^{-6}
356.0	5.0	10	−1.0	-0.24×10^{-3}
1510.0	0.3252	10	−1.0	0.50×10^{-4}

TABLE 1. A comparison with Cotton & Salwen's (1981) results. (Cotton & Salwen use $(R, \hat{\Omega})$ as the control parameters with $\hat{\Omega} = qR$.)

The resulting generalized eigenvalue problem was solved either by the QZ method using the IMSL subroutine EIGZC or by using the Inverse Power Iteration when a good guess of the eigenvalue is available. The results were compared with those from Cotton & Salwen (1981) who found the neutral points in $(R, q; m, k)$ space. Table 1 lists some combinations of $(R, q; k, m)$ for the neutral point found by Cotton & Salwen, i.e. points where they find the growth rates to be zero. We solved the linear eigenvlaue problem at the *same* parameters, and the resulting growth rates are also listed in table 1. They are less than 10^{-3}, which leads to three-figure accuracy for the combinations of parameters $(R, q; m, k)$, which is the reported accuracy in Cotton & Salwen (1981). In all the computations, 35 basis functions were found sufficient to give four-digit accuracy in the first three eigenvalues.

Our primary interest is to find the marginal stability curve, about which a weakly nonlinear stability analysis is to be made. In our computation, a point is said to be on the marginal stability curve when the absolute value of the growth rate is less than 10^{-4}; we believe that this growth rate criterion provides at least three-figure accuracy for the combinations of parameters $(R, q; m, k)$ on the marginal stability

curve. Figure 1 shows the marginal stability curve in the (R, q)-plane. In the limits of fast rotation and slow rotation, the limits found by Pedley (1969) and Mackrodt (1976) are respectively captured. The first two columns of table 2 give information for a collection of points on the marginal stability curve. They give the (R, q) pair on the marginal stability curve, and the axial wavenumber k of the marginally stable perturbation. The modes giving rise to the marginal stability all have an azimuthal wavenumber of $m = 1$. These modes are called 'bending modes' by Leibovich, Brown & Patel (1986), who point out that these are the only modes allowing particle deflection from the axis of the pipe, an important phenomenon observed in vortex breakdown.

In the study of the nonlinear evolution of the wave packet undertaken in the next section, the form of the dispersion relation near the marginal stability curve is needed. Near a point on the marginal stability curve, $(R_c, q_c; m = 1, k_c)$ for example, we have

$$\omega = \omega_0 + \omega_k(k-k_c) + \tfrac{1}{2}\omega_{kk}(k-k_c)^2 + \omega_R(R-R_c) + \omega_q(q-q_c) + \ldots, \tag{11}$$

where ω_0 is the eigenvalue of the linear problem calculated for parameters on the marginal stability curve; it is a real number. Since on the marginal stability curve, $(\mathrm{Im}\,\omega)_k = 0$, the group velocity $c_g = \omega_k$ is also real. The parameters $\omega_{kk}, \omega_R, \omega_q$ are generally complex.

To find the constants in the linear dispersion relation, we take the partial derivative of the linear problem with respect to k, R, q respectively. Let $\boldsymbol{M}_1$ denote the partial derivative of the matrix $\boldsymbol{M}$ with respect to its first argument, etc. We then have

$$\left.\begin{aligned} (-\mathrm{i}\omega_k \boldsymbol{M}_1 + \mathrm{i}\boldsymbol{M}_2)\boldsymbol{\Phi} &= -\boldsymbol{M}\boldsymbol{\Phi}_k, \\ (-\mathrm{i}\omega_R \boldsymbol{M}_1 + \boldsymbol{M}_4)\boldsymbol{\Phi} &= -\boldsymbol{M}\boldsymbol{\Phi}_R, \\ (-\mathrm{i}\omega_q \boldsymbol{M}_1 + \boldsymbol{M}_5)\boldsymbol{\Phi} &= -\boldsymbol{M}\boldsymbol{\Phi}_q. \end{aligned}\right\} \tag{12}$$

Since the matrix operator on the right-hand side is the same as the original linear equation, solvability conditions have to be satisfied in order for a solution of the above equations to exist. The solvability condition is

$$\langle \mathrm{LHS}, \boldsymbol{\Psi} \rangle = 0,$$

where LHS stands for the left-hand side of the equation, and $\boldsymbol{\Psi}$ is the solution of the linear algebraic problem adjoint to $\boldsymbol{M}\boldsymbol{\Phi} = 0$. The matrix for the adjoint problem is simply the Hermitian of $\boldsymbol{M}$. The inner product is defined by

$$\langle u, v \rangle = \sum_{i=1}^{n} u_i v_i^*, \tag{13}$$

where an asterisk represents the complex conjugate.

Applying the solvability condition to the above equations, we have

$$\left.\begin{aligned} \omega_k \langle \boldsymbol{M}_1 \boldsymbol{\Phi}, \boldsymbol{\Psi} \rangle &= \langle \boldsymbol{M}_2 \boldsymbol{\Phi}, \boldsymbol{\Psi} \rangle, \\ \mathrm{i}\omega_R \langle \boldsymbol{M}_1 \boldsymbol{\Phi}, \boldsymbol{\Psi} \rangle &= \langle \boldsymbol{M}_4 \boldsymbol{\Phi}, \boldsymbol{\Psi} \rangle, \\ \mathrm{i}\omega_q \langle \boldsymbol{M}_1 \boldsymbol{\Phi}, \boldsymbol{\Psi} \rangle &= \langle \boldsymbol{M}_4 \boldsymbol{\Phi}, \boldsymbol{\Psi} \rangle, \end{aligned}\right\} \tag{14}$$

which allows us to solve for $\omega_k, \omega_R, \omega_q$.

To find ω_{kk}, we take the derivative with respect to k once more to get

$$[-\mathrm{i}\omega_{kk}\boldsymbol{M}_1 - (\omega_k)^2 \boldsymbol{M}_{11} + 2\omega_k \boldsymbol{M}_{12} - \boldsymbol{M}_{22}]\boldsymbol{\Phi} + 2\mathrm{i}(-\omega_k \boldsymbol{M}_1 + \boldsymbol{M}_2)\boldsymbol{\Phi}_k = -\boldsymbol{M}\boldsymbol{\Phi}_{kk}. \tag{15}$$

Again, the solvability condition yields

$$\langle [-\tfrac{1}{2}(\omega_k)^2 \boldsymbol{M}_{11} + \omega_k \boldsymbol{M}_{12} - \tfrac{1}{2}\boldsymbol{M}_{22}]\boldsymbol{\Phi}, \boldsymbol{\Psi} \rangle + \mathrm{i}\langle [-\omega_k \boldsymbol{M}_1 + \boldsymbol{M}_2]\boldsymbol{\Phi}_k, \boldsymbol{\Psi} \rangle = \tfrac{1}{2}\mathrm{i}\omega_{kk} \langle \boldsymbol{M}_1 \boldsymbol{\Phi}, \boldsymbol{\Psi} \rangle \tag{16}$$

which can be solved for ω_{kk}.

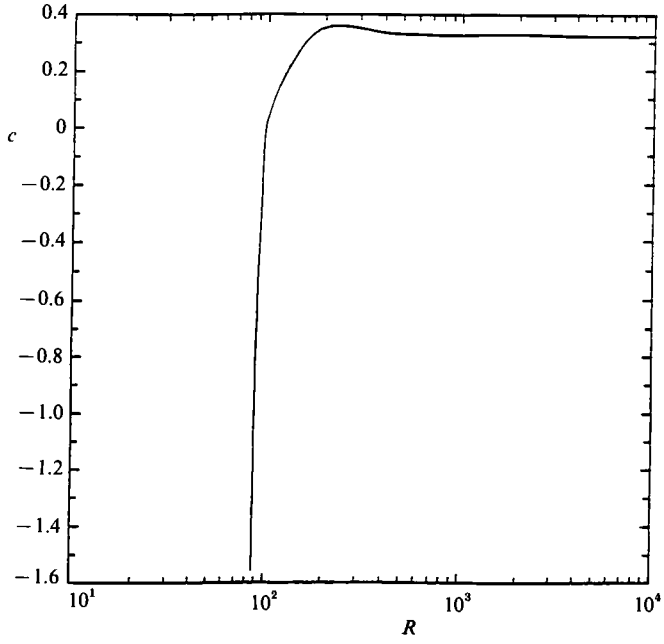

FIGURE 2. Axial phase speeds of neutral modes on the marginal stability boundary.

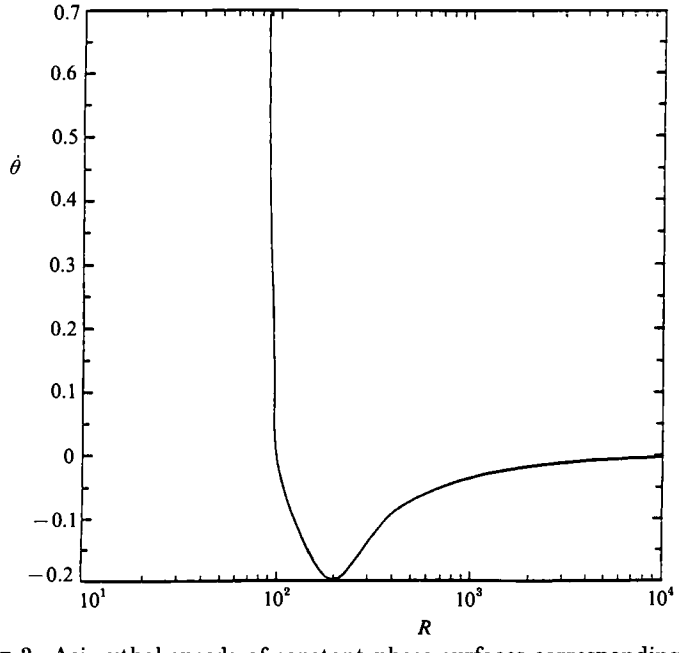

FIGURE 3. Azimuthal speeds of constant phase surfaces corresponding to figure 2.

Results from the above numerical calculation agreed with those from an alternative method, which used a second-order finite-difference representation for the derivatives. In this alternative approach, linear eigenvalue problems were solved repeatedly to provide the complex frequency at points needed to calculate the finite-difference representation. In figure 2, we show the values of $c = \omega/k$. The phase speed c gives the speed of a wavelet; and it is seen that c changes sign at $R \approx 95$. Below this

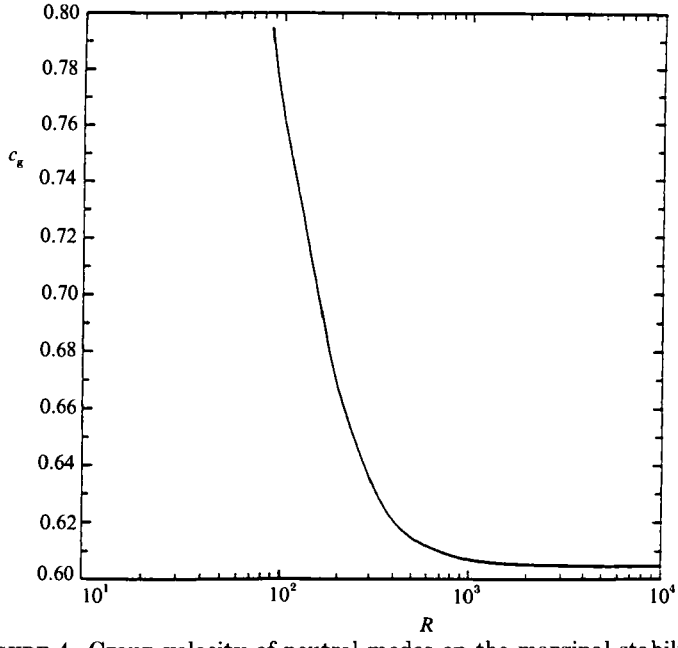

FIGURE 4. Group velocity of neutral modes on the marginal stability curve.

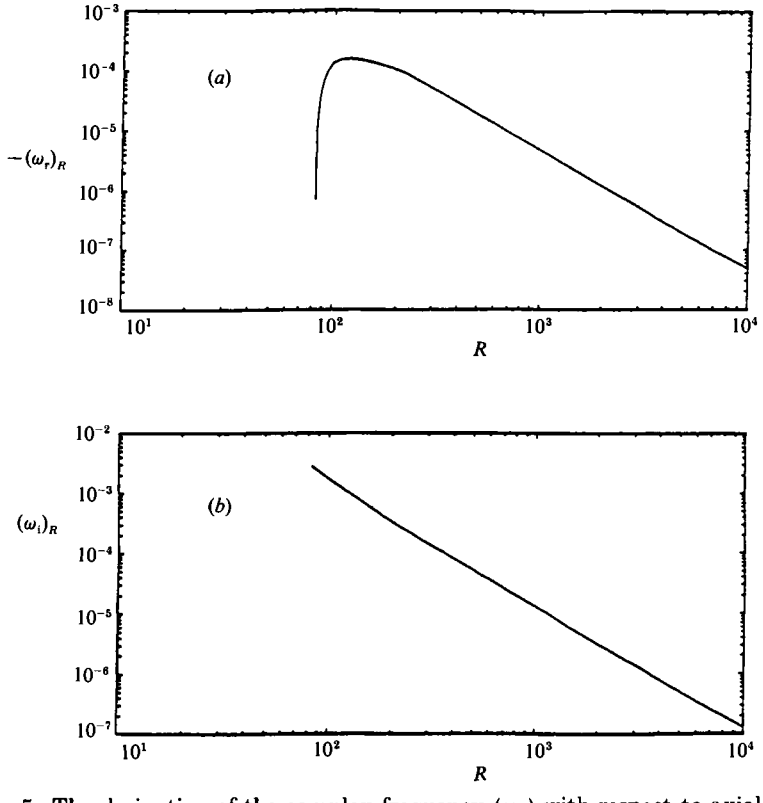

FIGURE 5. The derivative of the complex frequency (ω_R) with respect to axial Reynolds number for the neutral modes of figures 1–4. (*a*) Real part, (*b*) imaginary part.

value, c is negative, which means that wavelets propagate upstream. Above this valve, c is positive, and wavelets propagate downstream. In figure 3, we plot the values of ω. Since $m = 1$ on the marginal stability curve, $\dot{\theta} = \omega/m = \omega$ gives the angular velocity of the constant phase surface. In the laboratory frame, the constant phase surface rotates in the same direction as the base flow for $R < 95$ and rotates in the opposite direction for $R > 95$. Although the perturbation rotates in the same direction as the base flow for $R < 95$, the rotation is smaller than that of the base flow. Thus, in the frame rotating with the base flow, the perturbations rotate in a retrograde fashion, with direction opposite to that of base flow as observed in the laboratory frame. In figure 4, the values of $c_g = \mathrm{d}\omega/\mathrm{d}k$ are shown. It is seen that the group speed c_g is positive for all the points along the marginal stability curve, which means that the wave group and wave energy propagate downstream.

The values of ω_R, ω_q on the marginal stability curve are shown in figure 5 and figure 6 respectively. The imaginary part of both ω_R and ω_q are positive. Thus, on the marginal stability curve, if we increase R with q fixed or if we increase q with R fixed, the flow will pass the stability boundary with a non-zero speed and the bifurcation is strict.

The second derivative of the dispersion relation, ω_{kk}, is shown in figure 7. The magnitude of the imaginary part of this quantity determines the width of the wave band that is excited when we pass through the marginal stability curve.

4. Weakly nonlinear analysis

Let (R_c, q_c) be a point on the linear marginal stability curve. We study weakly supercritical parameter ranges, in which R is slightly greater than R_c or q is slightly greater than q_c or both. To be specific, we consider

$$R - R_c = \epsilon^2 \hat{R}, \quad q - q_c = \epsilon^2 \hat{q},$$

where $\epsilon \ll 1$ is a small parameter (see figure 8).

In the region of the parameters considered, a band of waves of width ϵ centred at the marginally stable wavenumber will become linearly unstable with a growth rate proportional to ϵ^2 (see figure 9). These waves will be allowed to be modulated both in time and in space. The modulation can be described in terms of the following slow variables:

$$T_1 = \epsilon t, \quad T_2 = \epsilon^2 t, \quad Z_1 = \epsilon z.$$

The perturbation field has the following expansion:

$$\hat{\boldsymbol{u}} = \epsilon \hat{\boldsymbol{u}}_1 + \epsilon^2 \hat{\boldsymbol{u}}_2 + \epsilon^3 \hat{\boldsymbol{u}}_3 + \ldots. \tag{17}$$

The rationale for the above scalings is standard: the width of the unstable wavenumber band is of order ϵ, which gives the slow spatial sale. These unstable waves have a phase speed which is different from the phase speed on the marginal stability curve by an amount of order ϵ, and a growth rate of order ϵ^2; thus we have the two slow timescales. The size of the perturbation is determined by the balance of the nonlinear term and the time growth term. Since the nonlinearity is quadratic, the nonlinear contribution comes in at the third order, thus we have

$$\mathrm{Im}\,(\omega)\,|\hat{\boldsymbol{u}}| \sim |\hat{\boldsymbol{u}}|^3,$$

which yields $|\hat{\boldsymbol{u}}| \sim \epsilon$.

It is well known that the wave system travels at the group speed. Thus, the number of slow variables may be reduced from three to two by transforming to a coordinate system which moves at the group speed. The new slow variables in such a system are:

$$Z = Z_1 - c_g T_1 = \epsilon(z - c_g t), \quad T = T_2 = \epsilon^2 t.$$

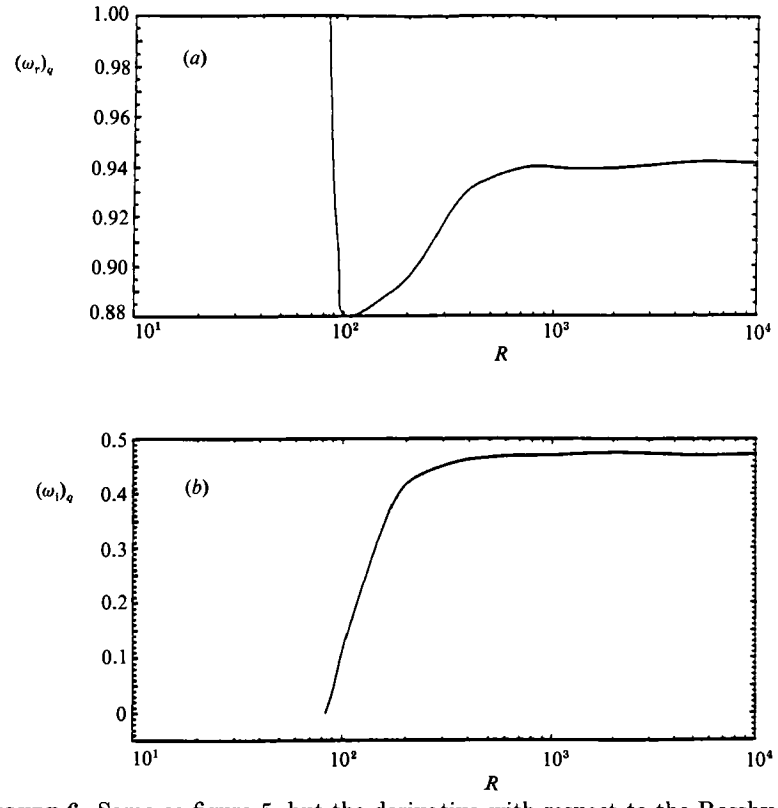

FIGURE 6. Same as figure 5, but the derivative with respect to the Rossby number (ω_q). (*a*) Real part, (*b*) imaginary part.

In the multiscale technique, we have the following transformation:

$$\frac{\partial}{\partial t} \to \frac{\partial}{\partial t} - \epsilon c_g \frac{\partial}{\partial Z} + \epsilon^2 \frac{\partial}{\partial T}, \qquad \frac{\partial}{\partial z} \to \frac{\partial}{\partial z} + \epsilon \frac{\partial}{\partial Z},$$

and thus

$$\begin{aligned} &\mathbf{L}\left(\frac{\partial}{\partial t}, \frac{\partial}{\partial z}, \frac{\partial}{\partial \theta}, \frac{\partial}{\partial r}; R, q\right) \\ &\quad \to \mathbf{L}\left(\frac{\partial}{\partial t} - \epsilon c_g \frac{\partial}{\partial Z} + \epsilon^2 \frac{\partial}{\partial T}, \frac{\partial}{\partial z} + \epsilon \frac{\partial}{\partial Z}, \frac{\partial}{\partial \theta}, \frac{\partial}{\partial r}; R_c + \epsilon^2 \hat{R}, q_c + \epsilon^2 \hat{q}\right) \\ &\quad = \mathbf{L}^{(0)} + \epsilon \mathbf{L}^{(1)} + \epsilon^2 \mathbf{L}^{(2)} + \ldots, \end{aligned}$$

where

$$\mathbf{L}^{(0)} = \mathbf{L}\left(\frac{\partial}{\partial t}, \frac{\partial}{\partial z}, \frac{\partial}{\partial \theta}, \frac{\partial}{\partial r}, R\right),$$

$$\mathbf{L}^{(1)} = -c_g \mathbf{L}_1 \frac{\partial}{\partial Z} + \mathbf{L}_2 \frac{\partial}{\partial Z},$$

$$\mathbf{L}^{(2)} = \tfrac{1}{2} c_g^2 \mathbf{L}_{11} \frac{\partial^2}{\partial Z^2} + \mathbf{L}_1 \frac{\partial}{\partial T} + \tfrac{1}{2} \mathbf{L}_{22} \frac{\partial^2}{\partial Z^2} - c_g \mathbf{L}_{12} \frac{\partial^2}{\partial Z^2} + \hat{R} \mathbf{L}_4 + \hat{q} \mathbf{L}_5.$$

Upon substituting the above into the governing equations, we have a series of equations for different orders of ϵ.

To $O(\epsilon^1)$

$$\mathbf{L}^{(0)} \hat{\boldsymbol{u}}_1 = 0. \tag{18}$$

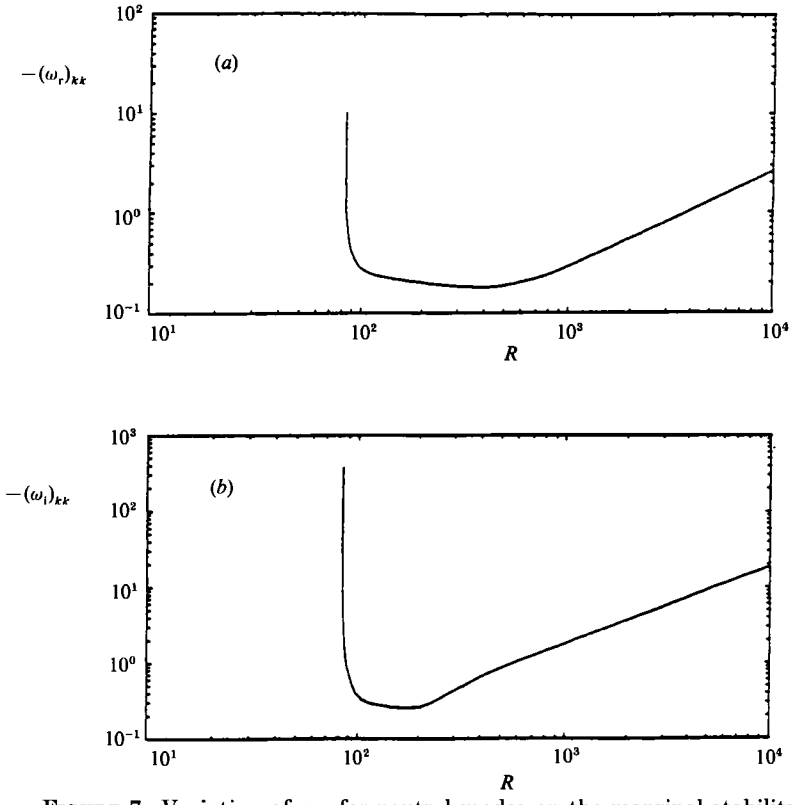

FIGURE 7. Variation of ω_{kk} for neutral modes on the marginal stability curve. (*a*) Real part, (*b*) imaginary part.

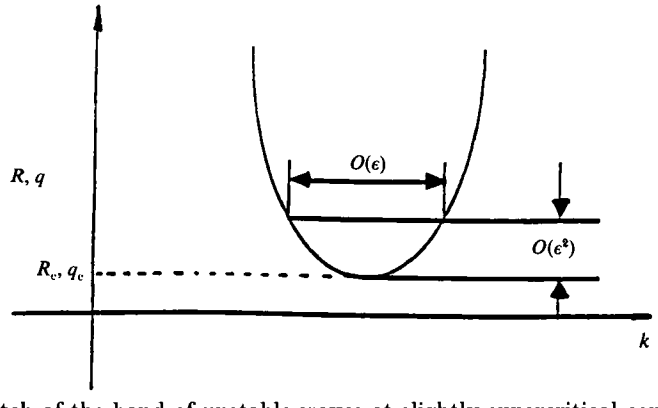

FIGURE 8. Sketch of the band of unstable waves at slightly supercritical conditions for which the weakly nonlinear analysis is done.

This is the linear problem we have treated and its solution is given by

$$\hat{\boldsymbol{u}}_1 = A\boldsymbol{\varphi}E + \text{c.c.}, \tag{19}$$

where the function $\boldsymbol{\varphi}$ is the same linear eigenfunction as was found previously; c.c. stands for the complex conjugate, for the physical perturbation field has to be real. Instead of being an arbitrary constant, the amplitude A is a function of the slow variables Z, T now, i.e.

$$A = A(Z, T).$$

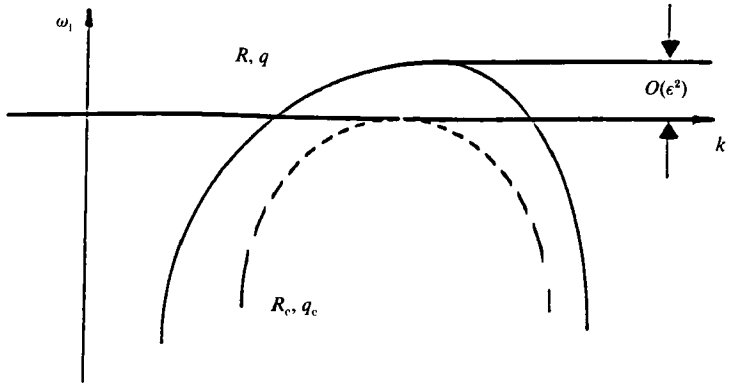

FIGURE 9. Sketch of the linear growth rates corresponding to figure 8.

To $O(\epsilon^2)$

$$\begin{aligned}\mathbf{L}^{(0)}\hat{\boldsymbol{u}}_2 &= \mathbf{N}(\hat{\boldsymbol{u}}_1,\hat{\boldsymbol{u}}_1)-\mathbf{L}^{(1)}\hat{\boldsymbol{u}}_1\\ &= A^2E^2\mathbf{N}(\boldsymbol{\varphi},\boldsymbol{\varphi})+|A|^2\mathbf{N}(\boldsymbol{\varphi},\boldsymbol{\varphi}^*)-\mathbf{L}^{(1)}AE\boldsymbol{\varphi}+\text{c.c.}.\end{aligned} \tag{20}$$

Because of the homogeneity of the operator $\mathbf{L}$ in the z,θ,t-directions, the solution of the above equation can be written as

$$\hat{\boldsymbol{u}}_2 = A^2E^2\boldsymbol{\varphi}_2+|A|^2\boldsymbol{\varphi}_0+\frac{\partial A}{\partial Z}E\boldsymbol{\varphi}_1+\text{c.c.}. \tag{21}$$

We then have

$$\left.\begin{aligned}\mathbf{L}\left(-2\mathrm{i}\omega, 2\mathrm{i}k, 2\mathrm{i}m, \frac{\partial}{\partial r}; R, q\right)\boldsymbol{\varphi}_2 &= \mathbf{N}(\boldsymbol{\varphi},\boldsymbol{\varphi}),\\ \mathbf{L}\left(0,0,0,\frac{\partial}{\partial r}; R, q\right)\boldsymbol{\varphi}_0 &= \mathbf{N}(\boldsymbol{\varphi},\boldsymbol{\varphi}^*),\\ \mathbf{L}\left(-\mathrm{i}\omega, \mathrm{i}k, \mathrm{i}m, \frac{\partial}{\partial r}; R, q\right)\boldsymbol{\varphi}_1 &= c_g\,\mathbf{L}_1\boldsymbol{\varphi}-\mathbf{L}_2\boldsymbol{\varphi}.\end{aligned}\right\} \tag{22}$$

The second harmonics term $\boldsymbol{\varphi}_2$ can be easily found, because the differential operator $\mathbf{L}(-2\mathrm{i}\omega, 2\mathrm{i}k, 2\mathrm{i}m, \partial/\partial r; R, q)$ is invertible. In the discretized algebraic problem, the matrix $\boldsymbol{M}(-2\mathrm{i}\omega, 2\mathrm{i}k, 2\mathrm{i}m; R, q)$ is invertible for $(R, q; k, m)$ on the marginal stability curve, so the discrete form of $\boldsymbol{\varphi}_2$ is readily found.

In finding the mean flow distortion term $\boldsymbol{\varphi}_0$, we found that the operator $\mathbf{L}(0,0,0,\partial/\partial r; R, q)$ is singular and the matrix $\boldsymbol{M}(0,0,0; R, q)$ cannot be inverted. However, this singularity was found to correspond to the fact that the pressure perturbation is indeterminate up to an arbitrary constant. Further investigation shows that the velocity components are decoupled from the pressure in this case. Although the pressure perturbation is not determined, the velocity perturbation in the mean flow distortion is determined, and could be easily found. Thus, the singularity in the operator $\mathbf{L}(0,0,0,\partial/\partial r; R, q)$ does not cause us any difficulty in carrying out the amplitude expansion, for the nonlinearity involves the velocity perturbations only.

If we had not assumed that the wave system travels at the group speed, and worked on the three slow variables Z_1, T_1, T_2, we would have found that the solvability condition for the third equation would lead to the result that the wave system travels at the group speed. Now, although $\mathbf{L}(-\mathrm{i}\omega, \mathrm{i}k, \mathrm{i}m, \partial/\partial r; R, q)$ is singular, $\boldsymbol{\varphi}_1$ can still be found because the right-hand side satisfies the solvability condition. The solution consists of two parts, the general solution of the homogeneous problem,

(R, q)	k	β	c_d	c_n	μ_n^2	N
(82.9, 20.0)	-2.5×10^{-2}	$(-0.565, -2.63\times10^{-3})$	-0.271×10^{-1}	0.466×10^{-2}	0.333	0.999
(82.9, 10.0)	-5.0×10^{-2}	$(-1.99, -1.94\times10^{-2})$	-0.545×10^{-1}	0.974×10^{-2}	0.333	0.999
(82.9, 8.0)	-6.2×10^{-2}	$(-2.85, -3.58\times10^{-2})$	-0.678×10^{-1}	0.125×10^{-1}	0.333	0.999
(83.1, 5.0)	-1.0×10^{-1}	$(-5.38, -0.121)$	-0.108	0.225×10^{-1}	0.332	0.997
(83.3, 4.0)	-1.2×10^{-1}	$(-6.76, -0.209)$	-0.134	0.309×10^{-1}	0.332	0.995
(83.5, 3.0)	-1.6×10^{-1}	$(-8.41, -0.391)$	-0.177	0.465×10^{-1}	0.331	0.991
(83.9, 2.0)	-2.4×10^{-1}	$(-10.17, -0.862)$	-0.259	0.847×10^{-1}	0.326	0.977
(86.9, 1.0)	-4.5×10^{-1}	$(-11.6, -2.61)$	-0.467	0.224	0.298	0.894
(90.0, 0.74)	-5.6×10^{-1}	$(-11.8, -3.89)$	-0.576	0.327	0.268	0.811
(95.0, 0.56)	-6.6×10^{-1}	$(-12.0, -5.44)$	-0.685	0.453	0.222	0.689
(100.0, 0.46)	-7.2×10^{-1}	$(-12.0, -6.60)$	-0.762	0.548	0.182	0.581
(200.0, 0.14)	-5.6×10^{-1}	$(-9.90, -8.27)$	-0.754	0.834	0.983×10^{-1}	0.370
$(400.0, 6.8\times10^{-2})$	-2.7×10^{-1}	$(-5.13, -3.98)$	-0.270	0.775	0.197	0.790
$(500.0, 5.4\times10^{-2})$	-2.2×10^{-1}	$(-4.10, -3.14)$	-0.219	0.766	0.207	0.831
$(600.0, 4.5\times10^{-2})$	-1.8×10^{-1}	$(-3.43, -2.62)$	-0.192	0.764	0.212	0.852
$(800.0, 3.4\times10^{-2})$	-1.3×10^{-1}	$(-2.56, -1.94)$	-0.167	0.758	0.216	0.873
$(1000.0, 2.7\times10^{-2})$	-1.1×10^{-1}	$(-1.98, -1.50)$	-0.159	0.755	0.218	0.879
$(2000.0, 1.3\times10^{-2})$	-5.3×10^{-1}	$(-0.982, -0.743)$	-0.148	0.756	0.220	0.887
$(10000.0, 2.7\times10^{-3})$	-1.1×10^{-2}	$(-0.199, -0.150)$	-0.140	0.753	0.221	0.894

TABLE 2. Wave packet data on the marginal stability curve

which is proportional to φ, and a particular solution which depends on the right-hand side. In the numerical computation, the particular solution was found by a singular-value decomposition.

To $O(\epsilon^3)$

$$\begin{aligned}\mathbf{L}^{(0)}\hat{u}_3 &= \mathbf{N}(\hat{u}_2,\hat{u}_1)+\mathbf{N}(\hat{u}_1,\hat{u}_2)-\mathbf{L}^{(1)}\hat{u}_2-\mathbf{L}^{(2)}\hat{u}_1\\ &= |A|^2AE[\mathbf{N}(\varphi_2,\varphi^*)+\mathbf{N}(\varphi_0,\varphi)+\mathbf{N}(\varphi,\varphi_0)+\mathbf{N}(\varphi^*,\varphi_2)]\\ &\quad -\mathbf{L}^{(1)}\frac{\partial A}{\partial Z}E\varphi_1+\mathbf{L}^{(2)}AE\varphi+\text{c.c.}+\text{n.s.t.},\end{aligned} \tag{23}$$

where n.s.t. stands for the non-secular terms.

Application of the solvability condition to (23) leads to the amplitude equation, which is given by

$$\frac{\partial A}{\partial T}-\tfrac{1}{2}\mathrm{i}\omega_{kk}\frac{\partial^2 A}{\partial Z^2}=-\mathrm{i}(\omega_R\hat{R}+\omega_q\hat{q})A+\beta|A|^2A. \tag{24}$$

This is the Ginzburg–Landau equation for the evolution of the amplitude of the wave system. This equation would reduce to the Stuart–Landau equation if we drop the spatial modulation term, which corresponds to the situation where only the simple wave with wavenumber k_c is considered.

In (24), β, the Landau constant, is calculated from

$$\beta=-\frac{\langle \boldsymbol{b},\boldsymbol{\Psi}\rangle}{\langle \boldsymbol{M}_1\boldsymbol{\Phi},\boldsymbol{\Psi}\rangle}, \tag{25}$$

where $\boldsymbol{b}$ is a vector, the components of which are the Chebyshev expansion of the nonlinear terms given by

$$r^2[\mathbf{N}(\varphi_2,\varphi^*)+\mathbf{N}(\varphi_0,\varphi)+\mathbf{N}(\varphi,\varphi_0)+\mathbf{N}(\varphi^*,\varphi_2)].$$

Again, the r^2 factor was used to multiply the Navier–Stokes equation to eliminate the coordinate singularity. The Landau constant found this way was in agreement with those listed in Mahalov & Leibovich (1989) which uses an entirely different numerical procedure.

The real part of the Landau constant determines the nature of bifurcation when the flow passes the marginal stability curve. If $\beta_r<0$, the bifurcation is supercritical, and if $\beta_r>0$, the bifurcation is subcritical. If the bifurcation is subcritical, the effect of the nonlinearity is destabilizing and a nonlinear equilibrium may be found in the regions where the linear analysis predicts stability, due to the nonlinear effect. In the case of the rotating pipe flow with large R, the critical q to render the flow marginally stable is very small (proportional to $O(R^{-1})$). If the bifurcation were subcritical, it is conceivable that bifurcated states of motion in the non-rotating pipe flow might be traced as the limit of the rotating pipe flow when the rotation rate goes to zero. This might shed light on the observed transition in the non-rotating pipe flow where the linear analysis predicts stability. However, the numerical calculations show that the bifurcation is supercritical at *all* points calculated along the marginal stability curve on the (R,q)-plane. The values of β for Reynolds number up to $R=10000$ are listed in table 2. Since the bifurcation is supercritical, nonlinear effects will be stabilizing. The region of interest will be where the linear analysis predicts instability and there will be competition between linear and nonlinear effects. This is the subject of the next section.

5. Modulated travelling wave solution and its linear stability

The Ginzburg–Landau equation arises in other fluid dynamics problems, and in other branches of the physical sciences. It describes the evolution of the amplitude of a wave system near the critical state. There are a number of studies of this equation, concerning the route to chaos that it reveals. Our interest here, more restricted, is to see whether the travelling wave solutions of the Ginzburg–Landau equation, appropriate to the marginal stability curve for rotating pipe flow, are linearly stable.

Let
$$\sigma = -\mathrm{i}(\omega_R \hat{R} + \omega_q \hat{q}). \tag{26}$$

The linearly unstable region we are studying is given by

$$\sigma_r \geqslant 0.$$

The Ginzburg–Landau equation may be normalized by the following transformation:

$$A = \alpha_A \exp(\mathrm{i}\sigma_i T)\hat{A}, \quad T = \alpha_T \tau, \quad Z = \alpha_Z \xi.$$

If we choose $\alpha_A = (-\sigma_r/\beta_r)^{\frac{1}{2}}$, $\alpha_T = \sigma_r^{-1}$, $\alpha_Z = (-\lambda_i/2\sigma_r)^{\frac{1}{2}}$, $\lambda = \omega_{kk}$

the Ginzburg–Landau equation becomes

$$\frac{\partial \hat{A}}{\partial \tau} - c_1 \frac{\partial^2 \hat{A}}{\partial \xi^2} = \hat{A} - c_2 |\hat{A}|^2 \hat{A}, \tag{27}$$

where
$$c_1 = 1 + \mathrm{i}c_d, \quad c_2 = 1 + \mathrm{i}c_n$$

and
$$c_d = \lambda_r/\lambda_i, \quad c_n = \beta_i/\beta_r.$$

c_d, c_n are the new independent parameters entering the Ginzburg–Landau equation. Their signs determine the nature of the solution. In the case of flow in a rotating pipe, the values of c_d, c_n along the marginal stability curve are listed in table 2. From the numerical results, it is seen that

$$c_d < 0, \quad \text{and} \quad c_n > 0.$$

The Ginzburg–Landau equation admits solutions of the following type:

$$\hat{A}_e = A_0 \exp[\mathrm{i}(\gamma_0 \tau + \mu_0 \xi)] \equiv A_0 E_0, \tag{28}$$

where A_0, γ_0 are related to μ_0 by

$$A_0 = (1 - \mu_0)^{\frac{1}{2}}, \quad \gamma_0 = -c_n + (c_n - c_d)\mu_0^2. \tag{29}$$

The solution thus represents a travelling wave. Since the above solution is in slow variables and A is the amplitude of the travelling wave in the fast variables, the solution represents a modulation of the wave given by the linear theory.

The family of travelling wave solutions of the Ginzburg–Landau equation is parametrized by μ_0. The range of μ_0 is confined to the region where the linear theory predicts instability, which gives

$$-1 \leqslant \mu_0 \leqslant 1.$$

When $\mu_0 = 0$, the resulting solution is called the Stokes solution, and corresponds to the modulation to the original travelling wave in time only.

For $\mu_0 = 0$, the travelling wave solution reduces to the Stokes solution. The condition for its instability is given by

$$N = 1 + c_d c_n < 0. \tag{30}$$

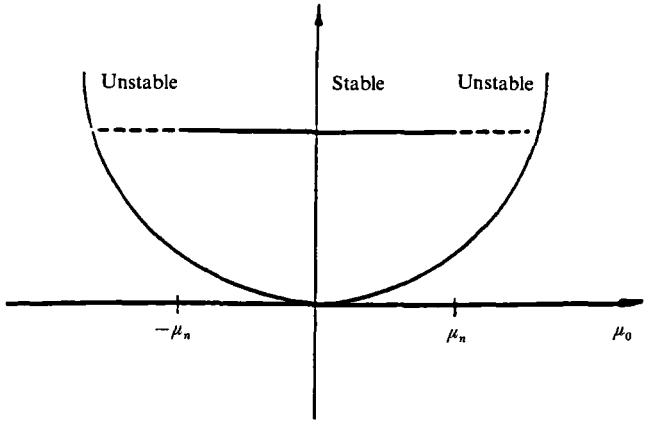

FIGURE 10. An illustration of window of stability for stable modulated waves, bounded by an Eckhaus instability. Instability is shown by broken lines, stability by the solid line.

This is the Newell condition (Newell 1974) for the instability of the spatially periodic wave with $k = k_c$ to sideband perturbations.

The values of N along the marginal stability curve are listed in table 2. It is found that $N > 0$ everywhere. Thus, the Newell condition for instability is not satisfied, all the waves with spatial wavenumber k_c are stable along the marginal stability curve.

The stability for general μ_0 was treated by Stuart & DiPrima (1978). The range of μ_0 for stability is

$$-\mu_n < \mu_0 < \mu_n,$$

where

$$\mu_n = \left(1 + \frac{2}{N} + \frac{2c_n^2}{N}\right)^{-\frac{1}{2}}.$$

the values of μ_n are also listed in table 2. The waves will be unstable if the wavenumber μ_0 is in the following window:

$$\mu_n^2 < \mu_0^2 \leqslant 1. \tag{31}$$

The regions of stability and instability are sketched in figure 10.

6. Discussion

We have studied the weakly nonlinear evolution of the wave system near the marginal stability curve for flow in a rotating pipe. As the marginal stability curve is crossed, the flow undergoes a supercritical Hopf bifurcation, and the steady-state base flow is replaced by a flow which is periodic in both time and space. This periodic flow is a travelling wave, modulated with μ_0 as the modulation wavenumber. The modulated travelling wave is unstable to perturbations of sideband type if the modulation wavenumber falls inside an instability window, the width of which varies on the marginal stability curve. In the fast rotation limit, the width is found to be the same as its counterpart in Bénard convection, and other flows where the principle of exchange of stabilities holds (see Eckhaus 1965). It is worth noting that the phase speed is very large in the fast rotation limit in rotating pipe flow.

Since we have restricted our stability study to perturbations of the sideband form, which is a rather special form, we have to interpret with reservation when our study shows that the solution is stable. The solution might be unstable to perturbations of other form in parameter regions where the solution is stable to the perturbations of the sideband type.

In regions where the travelling wave is unstable to perturbations of sideband type, it is of interest to know the further evolution of the motion. Keefe (1985), Sirovich & Newton (1986), Bernoff (1988) and others have carried out numerical computations for the evolution of the solutions of the Ginzburg–Landau equation. They find that the solution undergoes a sequence of transitions to limit cycles, tori, and chaos. These authors treat the Ginzburg–Landau equation in a parameter range in which the Stokes solution is unstable. In our case, the Stokes solution is stable, while the modulated travelling wave solutions are unstable. However, it is expected that the evolution would lead to a similar process of transition to chaos. Of course, this question can be answered with certainty only if a numerical computation is carried out for the solutions of the Ginzburg–Landau equations in flows applicable to our case.

Even if these unstable solutions are found to lead to chaos, their relevance to the transition to turbulence in a rotating pipe is still an open question, since the Navier–Stokes equations reduce to the Ginzburg–Landau equation only for small departures from the basic state. In the specific case of flow in a rotating pipe, a direct numerical simulation would be helpful in answering this question and establishing the link between the solutions of the Ginzburg–Landau equation and those of the Navier–Stokes equations.

This work was supported by the Air Force Office of Scientific Research under contract AFOSR-89-0346 monitored by Dr L. Sakell.

Appendix A. Operators L and N

In the cylindrical coordinate system (z, r, θ), the non-zero entries of $\mathbf{L}$ are

$$\left.\begin{aligned}
&\mathrm{L}_{(1,1)} = \frac{\partial}{\partial t} + (1-r^2)\frac{\partial}{\partial z} + q\frac{\partial}{\partial \theta} - \frac{1}{R}\nabla^2, \quad \mathrm{L}_{(1,3)} = -2r, \quad \mathrm{L}_{(1,4)} = \frac{\partial}{\partial z},\\
&\mathrm{L}_{(2,2)} = \frac{\partial}{\partial t} + (1-r^2)\frac{\partial}{\partial z} + q\frac{\partial}{\partial \theta} - \frac{1}{R}\left(\nabla^2 - \frac{1}{r^2}\right), \quad \mathrm{L}_{(2,3)} = 2q - \frac{1}{R}\frac{2}{r^2}\frac{\partial}{\partial \theta},\\
&\mathrm{L}_{(2,4)} = \frac{1}{r}\frac{\partial}{\partial \theta}, \quad \mathrm{L}_{(3,2)} = -2q + \frac{1}{R}\frac{2}{r^2}\frac{\partial}{\partial \theta},\\
&\mathrm{L}_{(3,3)} = \frac{\partial}{\partial t} + (1-r^2)\frac{\partial}{\partial z} + q\frac{\partial}{\partial \theta} - \frac{1}{R}\left(\nabla^2 - \frac{1}{r^2}\right), \quad \mathrm{L}_{(3,4)} = \frac{\partial}{\partial r},\\
&\mathrm{L}_{(4,1)} = \frac{\partial}{\partial z}, \quad \mathrm{L}_{(4,2)} = \frac{1}{r}\frac{\partial}{\partial \theta}, \quad \mathrm{L}_{(4,3)} = \frac{1}{r} + \frac{\partial}{\partial r},
\end{aligned}\right\} \tag{A 1}$$

and the non-zero entries of $\mathbf{N}$ are

$$\left.\begin{aligned}
&\mathrm{N}_1 = -\left(u\frac{\partial u}{\partial z} + \frac{v}{r}\frac{\partial u}{\partial \theta} + w\frac{\partial u}{\partial r}\right), \quad \mathrm{N}_2 = -\left(u\frac{\partial v}{\partial z} + \frac{v}{r}\frac{\partial v}{\partial \theta} + w\frac{\partial v}{\partial r} + \frac{vw}{r}\right),\\
&\mathrm{N}_3 = -\left(u\frac{\partial w}{\partial z} + \frac{v}{r}\frac{\partial w}{\partial \theta} + w\frac{\partial w}{\partial r} - \frac{vv}{r}\right),
\end{aligned}\right\} \tag{A 2}$$

where

$$\nabla^2 = \frac{\partial^2}{\partial z^2} + \frac{1}{r^2}\frac{\partial^2}{\partial \theta^2} + \frac{1}{r}\frac{\partial}{\partial r} + \frac{\partial^2}{\partial r^2}.$$

Appendix B. The matrices $\boldsymbol{A}$ and $\boldsymbol{B}$

The matrix $\boldsymbol{A}$ may be written

$$\boldsymbol{A} = \begin{bmatrix} \boldsymbol{A}_{11} & \boldsymbol{A}_{12} & \boldsymbol{A}_{13} & \boldsymbol{A}_{14} \\ \boldsymbol{A}_{21} & \boldsymbol{A}_{22} & \boldsymbol{A}_{23} & \boldsymbol{A}_{24} \\ \boldsymbol{A}_{31} & \boldsymbol{A}_{32} & \boldsymbol{A}_{33} & \boldsymbol{A}_{34} \\ \boldsymbol{A}_{41} & \boldsymbol{A}_{42} & \boldsymbol{A}_{43} & \boldsymbol{A}_{44} \end{bmatrix}.$$

Elements of the block matrix $\boldsymbol{A}_{11}$ are given by

$$\boldsymbol{A}_{11}(i,j) = \left\langle r^2 \mathbf{L}_{11}\left(0, -\mathrm{i}k, \mathrm{i}m, \frac{\partial}{\partial r}; R, q\right) T_i(y), T_j(y) \right\rangle,$$

where $y = 2r-1$. Similar expressions are obtained for $\boldsymbol{A}_{12}, \ldots, \boldsymbol{A}_{34}$. The elements of $\boldsymbol{A}_{41}$ are given by

$$\boldsymbol{A}_{41}(i,j) = \left\langle r \mathbf{L}_{11}\left(0, -\mathrm{i}k, \mathrm{i}m, \frac{\partial}{\partial r}; R, q\right) T_i(y), T_j(y) \right\rangle,$$

with similar expressions for $\boldsymbol{A}_{42}$, etc.

The matrix $\boldsymbol{B}$ may be written

$$\boldsymbol{B} = \begin{bmatrix} \boldsymbol{B}_{11} & \boldsymbol{B}_{12} & \boldsymbol{B}_{13} & \boldsymbol{B}_{14} \\ \boldsymbol{B}_{21} & \boldsymbol{B}_{22} & \boldsymbol{B}_{23} & \boldsymbol{B}_{24} \\ \boldsymbol{B}_{31} & \boldsymbol{B}_{32} & \boldsymbol{B}_{33} & \boldsymbol{B}_{34} \\ \boldsymbol{B}_{41} & \boldsymbol{B}_{42} & \boldsymbol{B}_{43} & \boldsymbol{B}_{44} \end{bmatrix},$$

with block matrix elements

$$\boldsymbol{B}_{11}(i,j) = \boldsymbol{B}_{22}(i,j) = \boldsymbol{B}_{33}(ij) = \langle r^2 T_i(y), T_j(y) \rangle$$

and all the other entries are zero.

The last rows of the block matrices are replaced by the equations obtained from enforcing the boundary conditions for the Chebyshev representation of the field.

REFERENCES

Akylas, T. R. & Demurger, J. P. 1984 The effect of rigid rotation on the finite-amplitude stability of pipe flow at high Reynolds number. *J. Fluid Mech.* **148**, 193–205.

Batchelor, G. K. & Gill, A. E. 1962 Analysis of the stability of axisymmetric jets. *J. Fluid Mech.* **14**, 529–551.

Bernoff, A. J. 1988 Slowly varying fully nonlinear wavetrains in the Ginzburg–Landau equation. *Physica* D **30**, 363–381.

Cotton, F. W. & Salwen, H. 1981 Linear stability of rotating Hagen–Poiseuille flow. *J. Fluid Mech.* **108**, 101–125.

Davey, A. 1978 On Itoh's finite amplitude stability theory for pipe flow. *J. Fluid Mech.* **86**, 695–703.

Davey, A. & Nguyen, H. P. F. 1971 Finite-amplitude stability of pipe flow. *J. Fluid Mech.* **45**, 701–720.

Eckhaus, W. 1965 *Studies in Non-Linear Stability Theory*. Springer.

Gill, A. E. 1965 On the stability of small disturbances to Poiseuille flow in a circular pipe. *J. Fluid Mech.* **21**, 145–172.

Herbert, T. 1983 On perturbation methods in nonlinear stability theory. *J. Fluid Mech.* **126**, 167–186.

ITOH, N. 1977 Nonlinear stability of parallel flows with subcritical Reynolds number. Part 2. Stability of pipe Poiseuille flow to finite axisymmetric disturbances. *J. Fluid Mech.* **82**, 469–479.

JOSEPH, D. D. & CARMI, S. 1969 Stability of Poiseuille flow in pipes, annuli, and channels. *Q. Appl. Maths* **26**, 575–599.

KEEFE, L. R. 1985 Dynamics of perturbed wavetrain solutions to the Ginzburg–Landau equation. *Stud. Appl. Maths* **73**, 91–153.

LANDMAN, M. J. 1990 Time-dependent helical waves in rotating pipe flow. *J. Fluid Mech.* **221**, 289–310.

LEIBOVICH, S., BROWN, S. N. & PATEL, Y. 1986 Bending waves on inviscid columnar vortices. *J. Fluid Mech.* **173**, 595–624.

MACKRODT, P. A. 1976 Stability of Hagen–Poiseuille flow with superimposed rigid rotation. *J. Fluid Mech.* **73**, 153–164.

MAHALOV, A. & LEIBOVICH, S. 1989 Weakly nonlinear expansion for viscous rotating Hagen–Poiseuille flow. *Bull. Am. Phys. Soc.* **34**, 2318.

MAHALOV, A., TITI, E. & LEIBOVICH, S. 1990 Invariant helical subspaces for the Navier–Stokes equations. *Arch. Rat. Mech. Anal.* **112**, 193–222.

MAHALOV, A. & LEIBOVICH, S. 1991 Multiple bifurcation of rotating pipe flow. *Theor. Comput. Fluid Mech.* (in press).

NEWELL, A. C. 1974 Envelope equations. *Lect. Appl. Maths* **15**, 157–163.

ORSZAG, S. A. & PATERA, A. T. 1983 Secondary instability of wall-bounded shear flows. *J. Fluid Mech.* **128**, 347–385.

PATERA, A. T. & ORSZAG, S. A. 1981 Finite amplitude stability of axisymmetric pipe flow. *J. Fluid Mech.* **112**, 467–474.

PEDLEY, T. J. 1968 On the instability of rapidly rotating shear flows to non-axisymmetric disturbances. *J. Fluid Mech.* **31**, 603–607.

PEDLEY, T. J. 1969 On the instability of viscous flow in a rapidly rotating pipe. *J. Fluid Mech.* **35**, 97–115.

REYNOLDS, O. 1883 An experimental investigation of the circumstances which determines whether the motion of water shall be direct or sinuous, and of the law of resistance in parallel channels. *Phil. Trans.* **174**, 935–982.

SALWEN, H. & GROSCH, C. E. 1972 The stability of Poiseuille flow in a pipe of circular cross-section. *J. Fluid Mech.* **54**, 93–112.

SIROVICH, L. & NEWTON, P. K. 1986 Periodic solutions of the Ginzburg–Landau equation. *Physica* D **21**, 115–125.

STEWARTSON, K. & STUART, J. T. 1971 Nonlinear instability theory for a wave system in plane Poiseuille flow. *J. Fluid Mech.* **48**, 529–545.

STUART, J. T. 1960 On the non-linear mechanics of wave disturbances in stable and unstable parallel flows. Part 1. *J. Fluid Mech.* **9**, 353–370.

STUART, J. T. & DIPRIMA, R. C. 1978 The Eckhaus and Benjamin–Feir resonance mechanisms. *Proc. R. Soc. Lond.* A **362**, 27–41.

TOPLOSKY, N. & AKYLAS, T. R. 1988 Nonlinear spiral waves in rotating pipe flow. *J. Fluid Mech.* **190**, 39–54.

WATSON, J. 1960 On the non-linear mechanics of wave disturbances in stable and unstable parallel flows. Part 2. The development of a solution for plane Poiseuille flow and for plane Couette flow. *J. Fluid Mech.* **9**, 371–389.